Restriction/Classification Cancelled

OCT 12 1954 RECD

CLASSIFICATION CANCELLED

CONFIDENTIAL

Copy 1
RM SL54J04

NACA RM SL54J04

Source of Acquisition
CASI Acquired

CLASSIFICATION CANCELLED
Authority NACA RESEARCH ABSTRACTS and Reclassification Notice No. 111.
Date 1/10/62 By

NACA

Restriction/Classification Cancelled

RESEARCH MEMORANDUM

for the

Bureau of Aeronautics, Department of the Navy

MEASUREMENT OF THE STATIC STABILITY AND CONTROL AND THE DAMPING DERIVATIVES OF A 0.13-SCALE MODEL OF THE CONVAIR XFY-1 AIRPLANE

TED NO. NACA DE 368

RA 411102

By Joseph L. Johnson, Jr.

Langley Aeronautical Laboratory
Langley Field, Va.

CLASSIFICATION CANCELLED
CLASSIFIED DOCUMENT

This material contains information affecting the National Defense of the United States within the meaning of the espionage laws, Title 18, U.S.C., Secs. 793 and 794, the transmission or revelation of which in any manner to an unauthorized person is prohibited by law.

NATIONAL ADVISORY COMMITTEE
FOR AERONAUTICS
WASHINGTON
OCT 7 1954

FILE COPY
To be returned to the files of the National Advisory Committee for Aeronautics Washington, D.C.

10

CLASSIFICATION CANCELLED
CONFIDENTIAL

CLASSIFICATION CANCELLED
CONFIDENTIAL

NATIONAL ADVISORY COMMITTEE FOR AERONAUTICS

RESEARCH MEMORANDUM

for the

Bureau of Aeronautics, Department of the Navy

MEASUREMENT OF THE STATIC STABILITY AND CONTROL AND THE DAMPING DERIVATIVES OF A 0.13-SCALE MODEL OF THE CONVAIR XFY-1 AIRPLANE

TED NO. NACA DE 368

By Joseph L. Johnson, Jr.

SUMMARY

An investigation has been conducted to determine the static stability and control and damping in roll and yaw of a 0.13-scale model of the Convair XFY-1 airplane with propellers off from 0° to 90° angle of attack. The tests showed that a slightly unstable pitch-up tendency occurred simultaneously with a break in the normal-force curve in the angle-of-attack range from about 27° to 36°. The top vertical tail contributed positive values of static directional stability and effective dihedral up to an angle of attack of about 35°. The bottom tail contributed positive values of static directional stability but negative values of effective dihedral throughout the angle-of-attack range. Effectiveness of the control surfaces decreased to very low values at the high angles of attack. The model had positive damping in yaw and damping in roll about the body axes over the angle-of-attack range but the damping in yaw decreased to about zero at 90° angle of attack.

INTRODUCTION

An investigation is being conducted by the NACA to provide information on which preliminary studies of the stability and handling qualities of vertically rising airplanes can be based. This investigation consists of static force tests and oscillation tests to measure the stability and

CONFIDENTIAL
CLASSIFICATION CANCELLED

control characteristics from 0° to 90° angle of attack of existing models of straight, sweptback, and delta wing airplanes which are generally representative of possible vertically rising airplane configurations. One such model having a 60° delta wing and vertical tail surfaces was investigated previously and the results reported in reference 1. As a continuation of this investigation, a 0.13-scale model of the Convair XFY-1 airplane has been tested with propellers and wing tip pods off and the results are presented herein.

In the present investigation measurements were made of the static stabililty, control effectiveness, and damping derivatives of the model from 0° to 90° angle of attack. The model was tested with vertical tails off, with top tail on, and with top and bottom tails on.

SYMBOLS

Unless otherwise noted, all forces and moments are referred to the system of body axes orginating at a center-of-gravity position of 16.5 percent of the mean aerodynamic chord and 2.6 percent of the mean aerodynamic chord above the longitudinal body axis. (See fig. 1.)

S	wing area, sq ft
$\bar{c}$	mean aerodynamic chord, ft
V	airspeed, ft/sec
b	wing span, ft
q	dynamic pressure, lb/sq ft
β	angle of sideslip, deg
ψ	angle of yaw, deg
ϕ	angle of bank, deg
α	angle of attack, $\tan^{-1}\frac{w}{u}$, deg
θ	angle of pitch, deg ($\theta = \alpha$ when ψ and ϕ are zero)
X	longitudinal force, positive in direction of X-axis, lb
Y	lateral force, positive in direction of Y-axis, lb

Z	normal force, positive in direction of Z-axis, lb
M	pitching moment, ft-lb
N	yawing moment, ft-lb
L	rolling moment, ft-lb
C_Z	normal-force coefficient, Z/qS
C_X	longitudinal-force coefficient, X/qS
C_Y	lateral-force coefficient, Y/qS
C_m	pitching-moment coefficient, $M/qS\bar{c}$
C_n	yawing-moment coefficient, N/qSb
C_l	rolling-moment coefficient, L/qSb

$C_{Y_\psi} = \partial C_Y/\partial\psi$ per deg

$C_{l_\psi} = \partial C_l/\partial\psi$ per deg

$C_{n_\psi} = \partial C_n/\partial\psi$ per deg

$C_{Y_\phi} = \partial C_Y/\partial\phi$ per deg

$C_{l_\phi} = \partial C_l/\partial\phi$ per deg

$C_{n_\phi} = \partial C_n/\partial\phi$ per deg

$C_{Y_\beta} = \partial C_Y/\partial\beta$ per deg

$C_{l_\beta} = \partial C_l/\partial\beta$ per deg

$C_{n_\beta} = \partial C_n/\partial\beta$ per deg

$$C_{n_r} = \frac{\partial C_n}{\partial\frac{rb}{2V}} \text{ per radian}$$

$$C_{l_p} = \frac{\partial C_l}{\partial\frac{pb}{2V}} \text{ per radian}$$

$C_{n_{\dot{\beta}}} = \dfrac{\partial C_n}{\partial \frac{\dot{\beta} b}{2V}}$ per radian

$C_{l_{\dot{\beta}}} = \dfrac{\partial C_l}{\partial \frac{\dot{\beta} b}{2V}}$ per radian

p	rolling angular velocity, radian/sec
r, $\dot{\psi}$	yawing angular velocity, radian/sec
$\dot{\beta}$	rate of change of angle of sideslip, radian/sec
δ_e	simultaneous up or down deflection of elevons (positive when deflected down), deg
δ_a	total differential deflection of elevons (positive when left surface is down and right surface is deflected up), deg
δ_r	rudder deflection, deg
ω	angular velocity, radian/sec
u, v, w	velocity components along the X, Y, and Z body axes, respectively, ft/sec
k	reduced-frequency parameter referred to mean aerodynamic chord of the model, $\omega\bar{c}/2V$

SYSTEM OF AXES

All the data obtained in this investigation are referred to the body axes. This system of axes was chosen rather than the stability axes because it is known that airplanes which have high yawing inertia and low rolling inertia tend to roll about the principal longitudinal axis of inertia which is generally very nearly alined with the X-body axis. It is believed, therefore, that the motions of such airplanes would be sensed by the pilot about the body axes of the airplane, particularly, at the very high angles of pitch.

The sequence by which the body axes are displaced from the tunnel reference axes determines the relationship of θ, ψ, and ϕ to α

and β. When the sequence of displacement is (1) pitching the model about the Y-axis through the angle θ, (2) yawing the model about the Z-axis through the angle ψ and, (3) rolling the model about the X-axis through the angle ϕ, the following relationships are found to exist:

$$\left.\begin{aligned} \tan \alpha &= \frac{w}{u} = \tan \theta \frac{\cos \phi}{\cos \psi} + \tan \psi \sin \phi \\ \sin \beta &= \frac{v}{V} = \sin \theta \sin \phi - \cos \theta \sin \psi \cos \phi \end{aligned}\right\} \tag{1}$$

Assuming that ϕ and ψ are small and only one of these angles is varied, the above relationship can be expressed as follows,

$$\left.\begin{aligned} \alpha &\approx \theta \\ \beta &\approx \phi \sin \theta \ (\psi = 0^{\circ}) \\ \beta &\approx -\psi \cos \theta \ (\phi = 0^{\circ}) \end{aligned}\right\} \tag{2}$$

The sideslip derivatives C_{Y_β}, C_{n_β}, and C_{l_β} can be determined from the static roll data and static yaw data by using the above relations to give the following expressions,

$$\left.\begin{aligned} C_{Y_\beta} &\approx \frac{C_{Y_\phi}}{\sin \theta} \approx \frac{-C_{Y_\psi}}{\cos \theta} \\ C_{n_\beta} &\approx \frac{C_{n_\phi}}{\sin \theta} \approx \frac{-C_{n_\psi}}{\cos \theta} \\ C_{l_\beta} &\approx \frac{C_{l_\phi}}{\sin \theta} \approx \frac{-C_{l_\psi}}{\cos \theta} \end{aligned}\right\} \tag{3}$$

In the free-to-damp oscillation method used to obtain the damping derivatives, the total measured damping in yaw includes the damping produced by the yawing velocity C_{n_r} and the damping produced by the rate of change in the angle of sideslip $C_{n_{\dot{\beta}}}$. At 0° angle of pitch, the total damping in yaw is expressed as $C_{n_r} - C_{n_{\dot{\beta}}}$. As the pitch angle is

changed from 0° the relation between $\dot{\beta}$ and $\dot{\psi}$ is determined from equation (2) as $\dot{\beta} = -\dot{\psi} \cos \theta$. The expression for the total damping for any angle of pitch is, therefore,

$$C_{n_r} - C_{n_{\dot{\beta}}} \cos \theta \tag{4}$$

In a similar manner, the total damping in roll is shown to be:

$$C_{l_p} + C_{l_{\dot{\beta}}} \sin \theta \tag{5}$$

APPARATUS AND MODEL

The static force tests and oscillation tests were conducted in the Langley free-flight tunnel which is a low-speed tunnel with a 12-foot octagonal test section. The tunnel was designed primarily for flying dynamically scaled models but force testing and free-to-damp oscillation equipment has been installed so that the aerodynamic characteristics of models can be obtained.

Static force tests and free-to-damp oscillation tests were made using a sting-type support system. A complete description of the static and oscillation equipment used in these tests is given in reference 1. Photographs of the model mounted on the oscillation apparatus are shown in figure 2.

A three-view drawing of the model is shown in figure 3 and table I gives the dimensional characteristics of the model. All tests were made with propellers and wing tip pods off.

TESTS

Force tests were made to determine the static longitudinal and lateral stability and control characteristics of the model from 0° to 90° angle of pitch. The model was tested with vertical tails off, with top tail on, and with top and bottom tails on. All static and damping tests were run at a dynamic pressure of about 3.80 pounds per square foot which corresponds to a tunnel velocity of about 57.3 feet per second and to a test Reynolds number of about 740,000 based on the mean aerodynamic chord of 2.03 feet.

The free-to-damp oscillation tests were made by the method described in reference 1 to determine the damping-in-yaw and damping-in-roll parameters from 0° to 90° angle of pitch for the same configurations tested in the static condition.

No attempt was made in this investigation to determine the effect of changes in amplitude or frequency of the oscillation on the lateral damping. All the oscillation tests were made at a frequency of about 1.0 cycle per second which corresponds to a reduced-frequency parameter k of 0.111 based on the mean aerodynamic chord of 2.03 feet. For all of the oscillation tests the model was displaced in yaw or roll about 30° before being released and allowed to damp to 0° amplitude. The envelopes of the oscillations were plotted on semilogarithmic paper and were found to be fairly linear through the amplitude range investigated except for small amplitudes where the tunnel turbulence caused the data to be erratic. Because of the nonlinearity of the data at the small amplitudes, the logarithmic decrements or damping factors used to determine the damping derivatives of this investigation were obtained from the slopes of the envelope curves for amplitudes above approximately $\pm 2^{\circ}$ or $\pm 3^{\circ}$.

RESULTS AND DISCUSSION

Longitudinal Stability and Control Characteristics

The longitudinal stability and control characteristics are presented in figure 4. These data show that the model was statically longitudinally stable except for angles of pitch from about 27° to 36°. In this range a slightly unstable pitch-up tendency occurred simultaneously with a break in the normal-force curve.

The elevators remained effective over the angle-of-pitch range but the effectiveness decreased at the higher angles of pitch.

Lateral Stability and Control Characteristics

The variations of the lateral-force and moment coefficients with ψ and ϕ are shown in figures 5 and 6, respectively, for the three configurations tested. The variations with pitch angle of the yawing-moment and rolling-moment coefficients at zero ψ and ϕ which were obtained from the data of figures 5 and 6 are presented in figure 7. This figure shows that large and inconsistent out-of-trim moments were obtained at some angles of pitch. These out-of-trim moments are believed to result from the asymmetrical shedding of vortices generated by the nose of the fuselage. A similar effect was found in the investigation

of reference 1. The fact that the out-of-trim moments obtained from figure 5 do not agree with those obtained from figure 6 is believed to be significant only as an indication of the inconsistency of the data which made it virtually impossible to verify data with check tests.

Static stability derivatives.- The static yaw and roll stability derivatives are presented in figures 8 and 9, respectively. These derivatives were obtained from the data of figures 5 and 6 for amplitudes of ψ and ϕ of $\pm 5^{\circ}$. The sideslip derivatives presented in figure 10 were obtained from the static yaw and static roll derivatives by using the relationships presented in a preceding section for transforming angles of ϕ and ψ into β. The sideslip derivatives were obtained from the yaw data for angles of pitch from 0° to 60° and from the roll data for angles of pitch from 40° to 90°.

The sideslip derivatives of figure 10 show that the wing-fuselage combination was directionally unstable over most of the angle-of-pitch range but that the instability generally decreased with increasing angle of pitch. The contribution of the vertical tails to the directional stability was approximately constant up to about 20° angle of pitch and then decreased. The bottom tail contributed some directional stability throughout the angle-of-pitch range but the top tail became destabilizing at an angle of pitch of about 35°.

The effective dihedral of the wing-fuselage configuration was positive $-C_{l_\beta}$ except for angles of pitch near 20°. The top vertical tail contributed positive values of effective dihedral up to an angle of pitch of 35°. The bottom tail decreased the positive effective dihedral over the angle-of-pitch range.

Lateral control.- The aileron and rudder effectiveness data are presented in figures 11(a) and 11(b), respectively. The data of these figures show that the ailerons maintained positive rolling power over the angle-of-pitch range investigated but the effectiveness decreased rapidly at the higher angles of pitch. The adverse yawing moments produced by the ailerons increased rapidly for angles of pitch from about 15° to 40° and then decreased.

The yawing moment produced by the rudder of the top vertical tail (fig. 11(b)) decreased to zero at about 50° angle of pitch. With both tails on, the rudder effectiveness was maintained throughout the angle-of-pitch range although the effectiveness decreased rapidly above about 24° angle of pitch. Above an angle of pitch of about 34°, a deflection of 20° of both rudders was incapable of trimming out the adverse yawing moments produced by an aileron deflection of $\pm 30^{\circ}$. The rudder of the top vertical tail produced fairly large adverse rolling moments up to about 45° angle of pitch.

Damping derivatives.- Values of the damping-in-roll derivative $C_{l_p} + C_{l_{\dot{\beta}}} \sin \theta$ and the damping-in-yaw derivative $C_{n_r} - C_{n_{\dot{\beta}}} \cos \theta$ measured relative to the body axis are presented in figure 12.

For three configurations tested, the damping in roll increased as the angle of pitch was increased up to about 20° or 25° and then decreased. At the higher angles of pitch the damping-in-roll increased again and at 90° was generaly similar to that at 0° angle of pitch. The maximum damping in roll occurred for the tail-off configuration at about 25° angle of pitch. The rapid increase in damping in roll at the lower angles of pitch, particularly for the tail-off configuration, is attributed to the damping term $C_{l_{\dot{\beta}}} \sin \theta$ which was measured as a part of the total damping in roll in the oscillation tests. A detailed explanation of this term is given in reference 1. The top vertical tail produced damping in roll over the angle-of-pitch range except for angles of pitch from about 15° to 37°. The bottom tail provided damping up to about 50° angle of pitch.

The damping in yaw of the tail-off configuration remained relatively small over the angle-of-pitch range and decreased to about zero at 90° angle of pitch. These low values of damping indicate that the damping term $C_{n_{\dot{\beta}}} \cos \theta$ was much less significant than for the model of reference 1. The vertical tails contributed about a constant increment of damping up to an angle of pitch of about 40° and then their effectiveness decreased to zero at 90° angle of pitch.

The damping derivatives of figure 12 up to an angle of attack of 25° are replotted in figure 13 together with values of C_{n_r} and C_{l_p} from references 2 and 3. The data obtained from these references were measured by the rolling and yawing flow techniques about the stability axes on a model of the Convair XFY-1 airplane in the Langley stability tunnel. The model used in these tests was equipped with wing tip pods and because of these wing tip pods the span and area used in working up the data were slightly different than the values used for the present model. In addition, the vertical tail configurations for the two models were not the same and there were also some other slight differences in the geometry of the two models. Because of these differences, the data of figure 13 do not afford a direct indication of the effect of changing from the stability axis to the body axis and from rolling and yawing derivatives to oscillation derivatives.

A comparison of the damping-in-roll derivatives about the two systems of axes shows that, at zero angle of attack, the two sets of data are in fair agreement. With an increase in angle of attack, however, the damping in roll decreased about the stability axis whereas it increased about the body axis. As previously mentioned, this increase in damping is believed to be associated with the damping term $C_{l_{\dot{\beta}}} \sin \theta$ which apparently increased rapidly in this angle-of-attack range.

The damping-in-yaw derivatives are only in fair agreement but in general the variations of the derivatives with angle of attack for the two sets of data are not greatly different. The vertical tails of the free-flight-tunnel model contributed a greater increment of damping than those of the stability tunnel model. This greater tail effectiveness for the free-flight-tunnel model also occurred in about the same proportion in the case of the static directional stability parameter C_{n_β} (see ref. 4 and fig. 10 of this report).

SUMMARY OF RESULTS

The following results were obtained from the investigation of the 0.13-scale model of the Convair XFY-1 airplane with propellers off for the angle-of-pitch range from 0° to 90°.

1. A slightly unstable pitch-up tendency occurred simultaneously with a break in the normal-force curve in the angle-of-pitch range from about 27° to 36°.

2. The top vertical tail contributed positive values of static directional stability and effective dihedral up to an angle of pitch of about 35°. The bottom vertical tail contributed positive values of static directional stability but negative values of effective dihedral throughout the angle-of-pitch range.

3. The elevons were effective as ailerons or elevators over the angle-of-pitch range although their effectiveness decreased at the higher angles of pitch. The rudder of the top tail was ineffective for angles of pitch above 50° but the rudder effectiveness of the bottom tail was maintained throughout the angle-of-pitch range.

4. The model had positive damping in roll and damping in yaw about the body axes over the angle-of-pitch range but the damping in yaw decreased to about zero at 90° angle of pitch.

Langley Aeronautical Laboratory,
National Advisory Committee for Aeronautics,
Langley Field, Va., September 17, 1954.

Joseph L. Johnson Jr.
Joseph L. Johnson, Jr.
Aeronautical Research Scientist

Approved: Charles H. Zimmerman
for Thomas A. Harris
Chief of Stability Research Division

eba

REFERENCES

1. Hewes, Donald E.: Low-Speed Measurement of the Static Stability and Damping Derivatives of a 60° Delta-Wing Model for Angles of Attack of 0° to 90°. NACA RM L54G22a, 1954.

2. Queijo, M. J., Wolhart, Walter D., and Fletcher, H. S.: Wind-Tunnel Investigation at Low Speed of the Rolling Stability Derivatives of a 1/9-Scale Powered Model of the Convair XFY-1 Vertically Rising Airplane - TED No. NACA DE 373. NACA RM SL53E13, Bur. Aero., 1953.

3. Queijo, M. J., Wolhart, W. D., and Fletcher, H. S.: Wind-Tunnel Investigation at Low Speed of the Yawing Stability Derivatives of a 1/9-Scale Powered Model of the Convair XFY-1 Vertically Rising Airplane - TED No. NACA DE 373. NACA RM SL53D01, Bur. Aero., 1953.

4. Queijo, M. J., Wolhart, W. D., and Fletcher, H. S.: Wind-Tunnel Investigation at Low Speed of the Static Longitudinal and Lateral Stability Characteristics of a 1/9-Scale Powered Model of the Convair XFY-1 Vertically Rising Airplane - TED No. NACA DE 373. NACA RM SL53B20, Bur. Aero., 1953.

TABLE I.- GEOMETRIC CHARACTERISTICS OF THE MODEL

Wing (modified triangular plan form):	
Sweepback, leading edge, deg	55
Airfoil section	NACA 63-009 modified
Aspect ratio	1.75
Taper ratio	0.232
Area (total to center line), sq in.	812.00
Span, in.	37.66
Mean aerodynamic chord, in.	24.34
Span of elevon (each), in.	15.37
Chord of elevon, in.	2.92
Dihedral angle, deg	0
Fuselage length, in.	45.40
Vertical tails (modified triangular plan form):	
Sweepback, leading edge, deg	40
Airfoil section	NACA 63-009 modified
Aspect ratio	3.18
Area (total to center line), sq in.	397.88
Span, in.	34.73
Mean aerodynamic chord, in.	13.07
Span of top rudder, in.	14.13
Span of bottom rudder, in.	11.13
Chord of rudders, in.	2.85

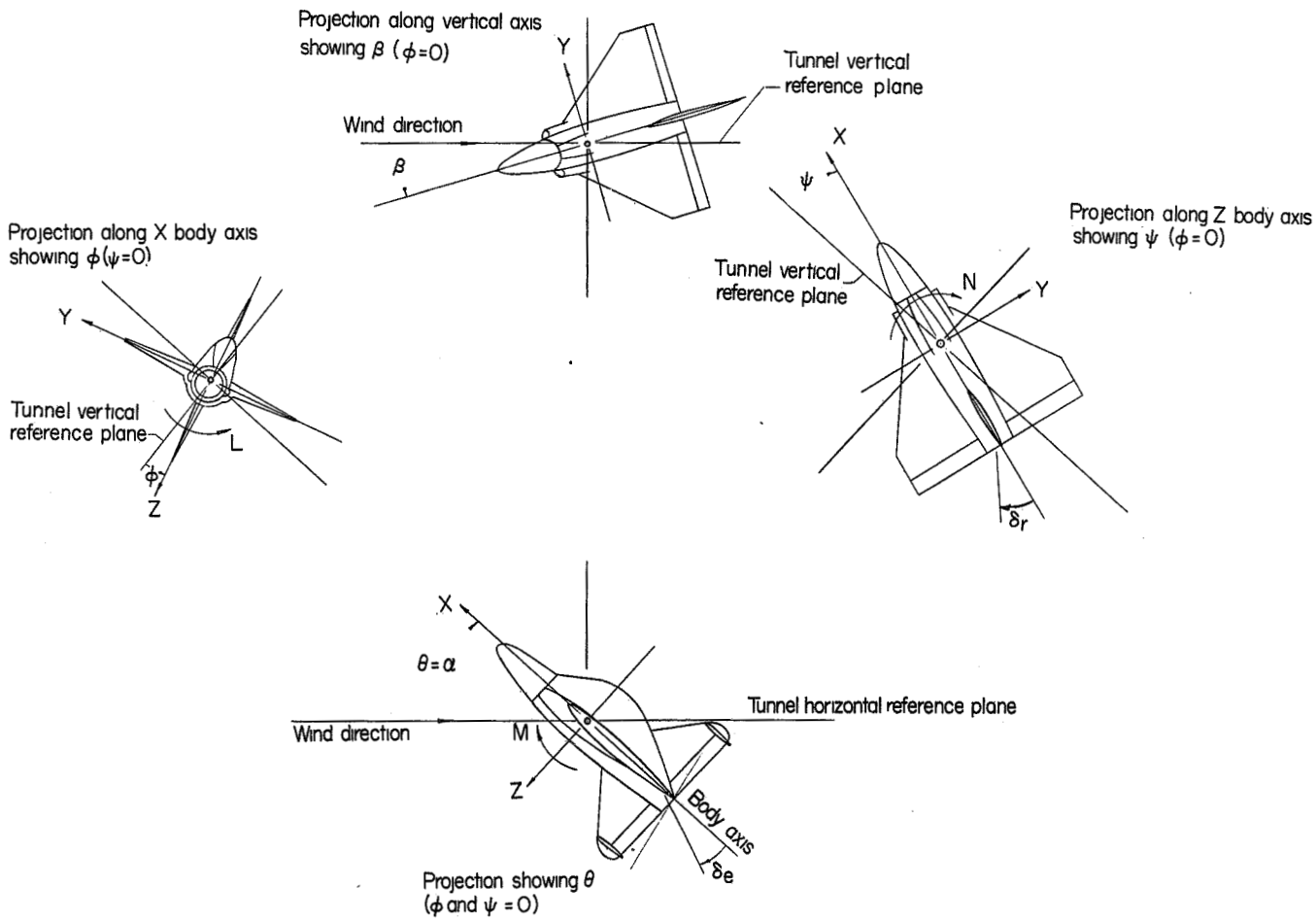

Figure 1.- The body system of axes. Arrows indicate positive directions of moments, forces, and angles. This system of axes is defined as an orthogonal system having the origin at the center of gravity and in which the X-axis is in the plane of symmetry and alined with the longitudinal axis of the fuselage, the Z-axis is in the plane of symmetry and perpendicular to the X-axis, and the Y-axis is perpendicular to the plane of symmetry.

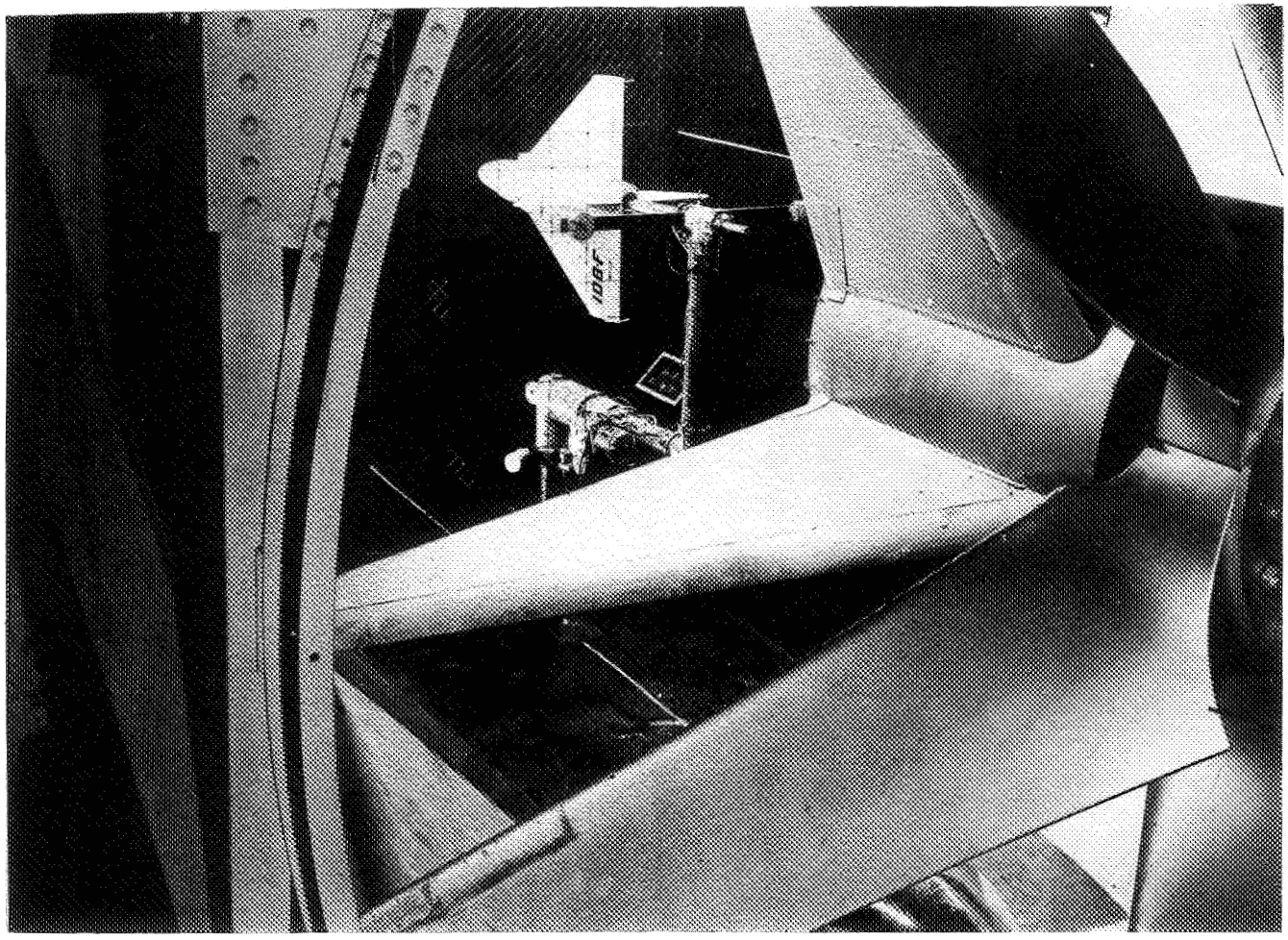

L-83391

(a) Model mounted for damping-in-roll tests.

Figure 2.- Photographs of model mounted on dynamic test equipment.

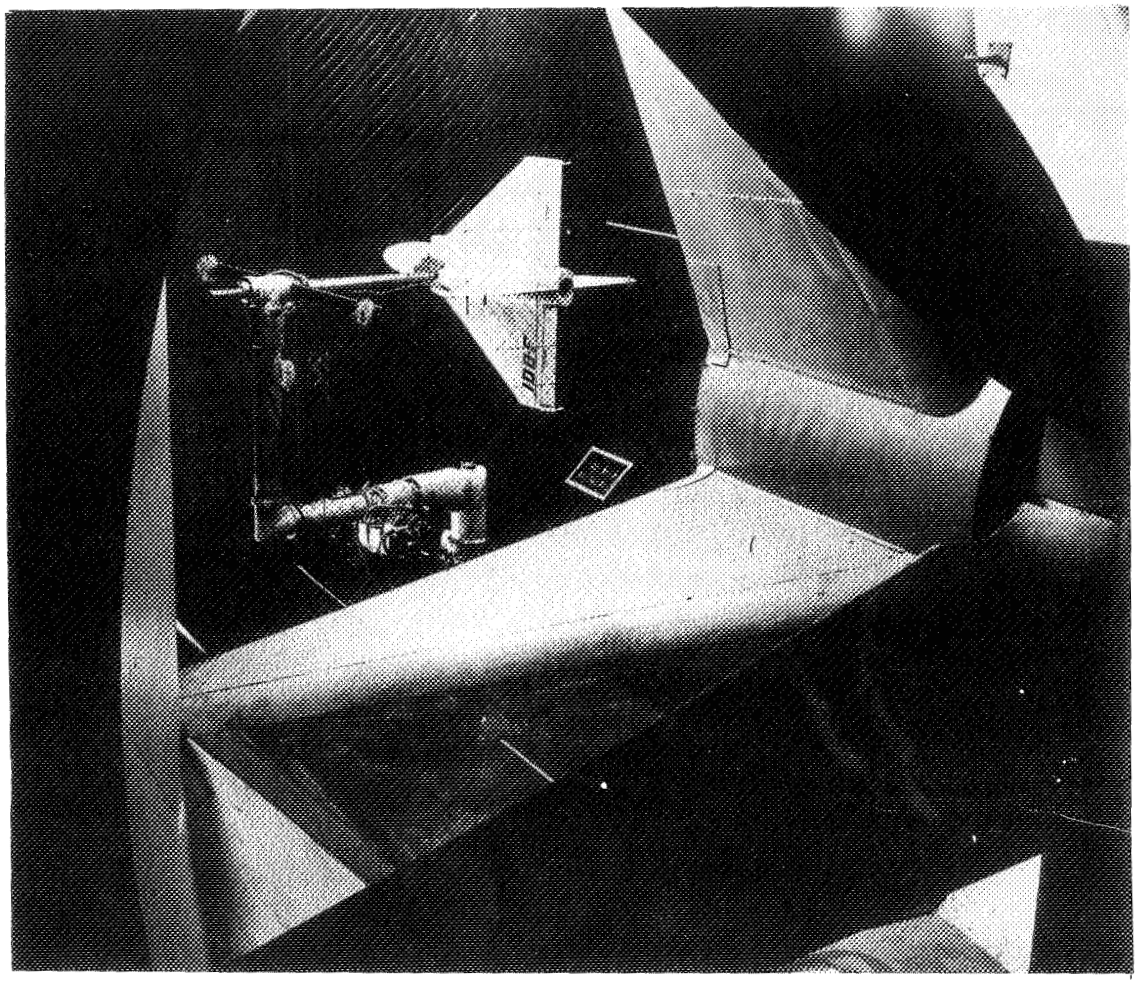

L-83388

(b) Model mounted for damping-in-yaw tests.

Figure 2.- Concluded.

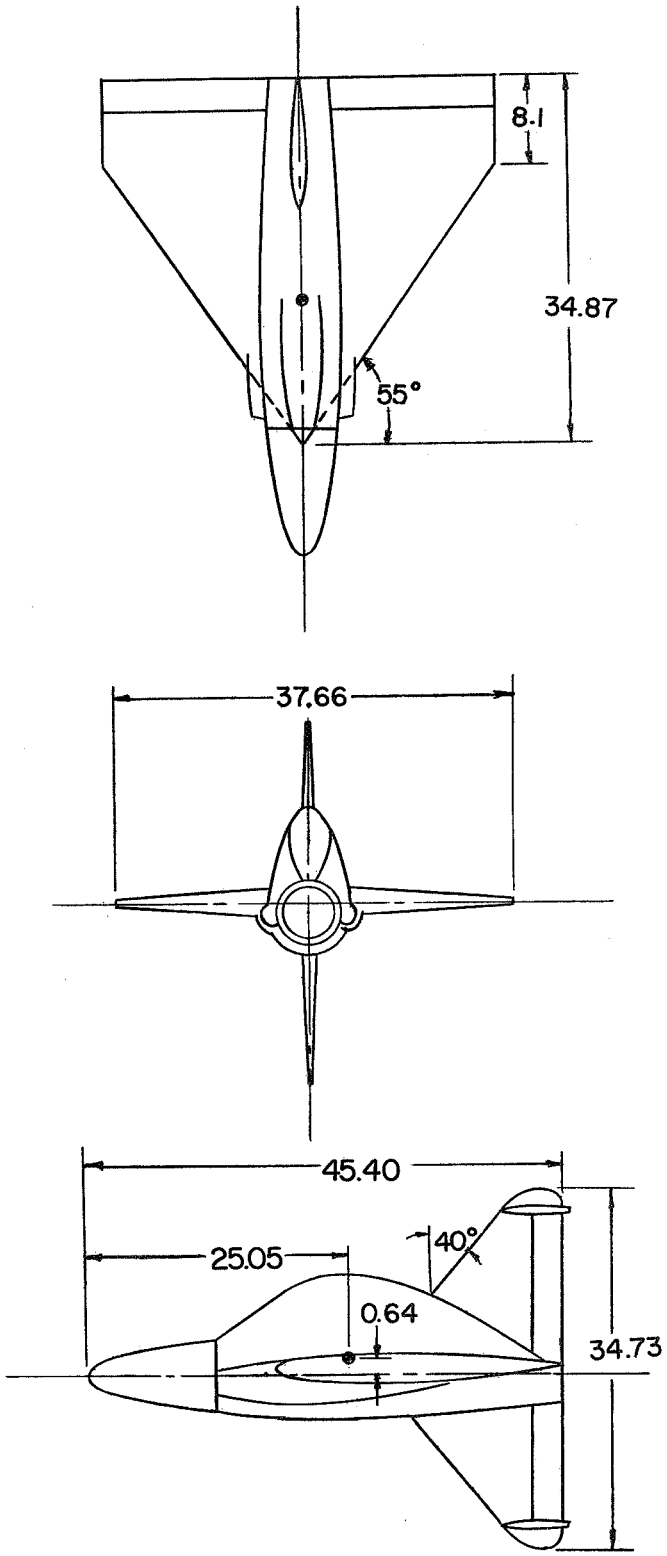

Figure 3.- Sketch of the 0.13-scale model used in the investigation. All dimensions are in inches.

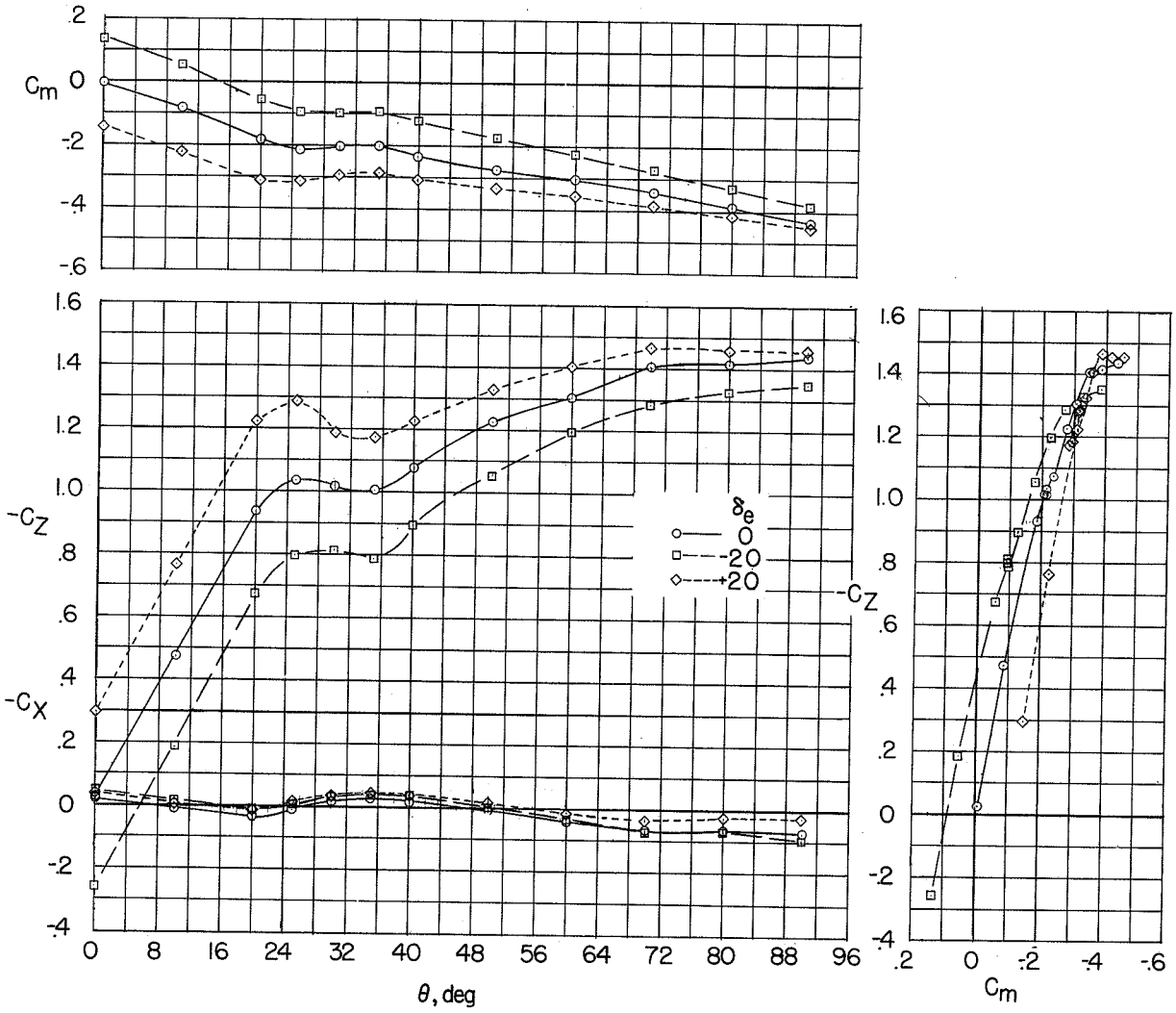

Figure 4.- Static longitudinal stability and control characteristics of the model. $\beta = 0^{\circ}$.

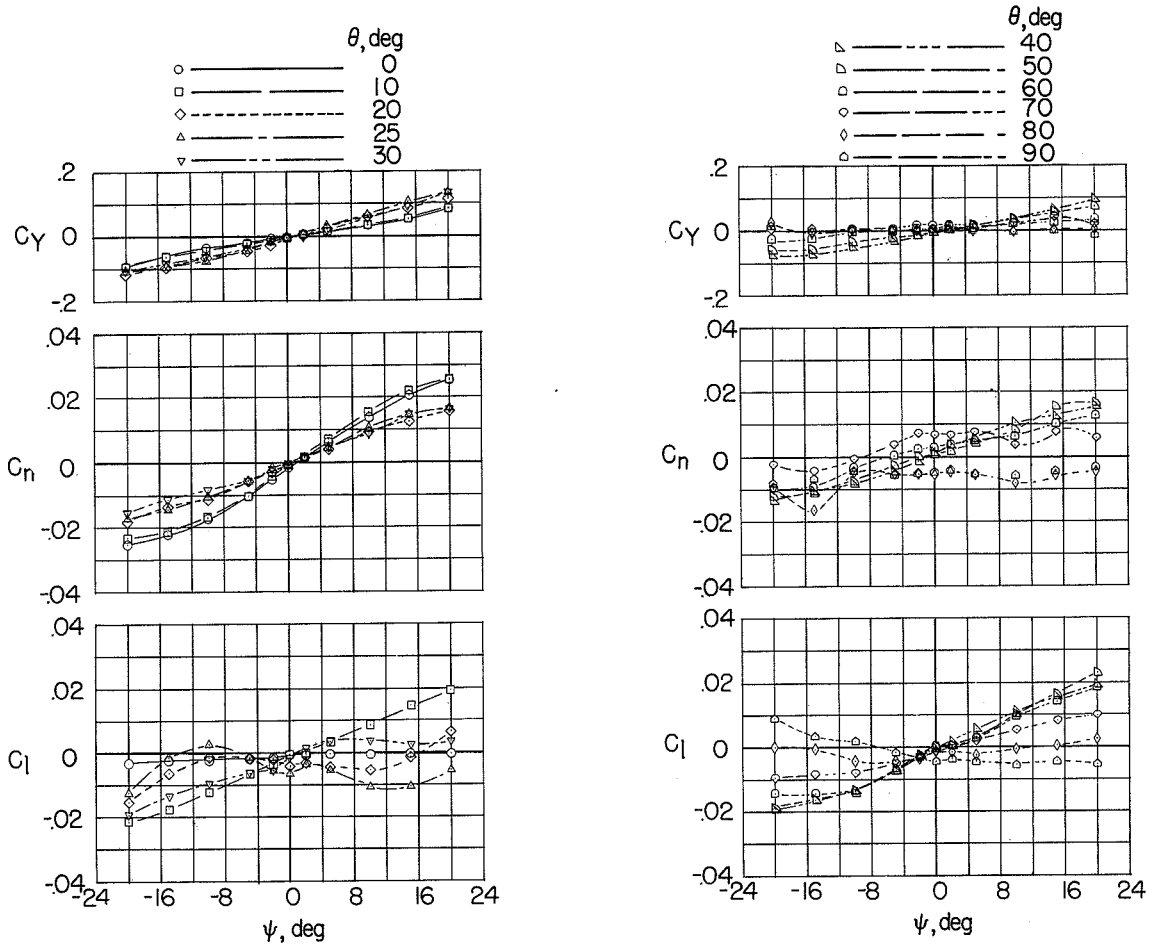

(a) Vertical tails off.

Figure 5.- Variation of the static lateral stability coefficients with angle of yaw. $\phi = 0^{\circ}$.

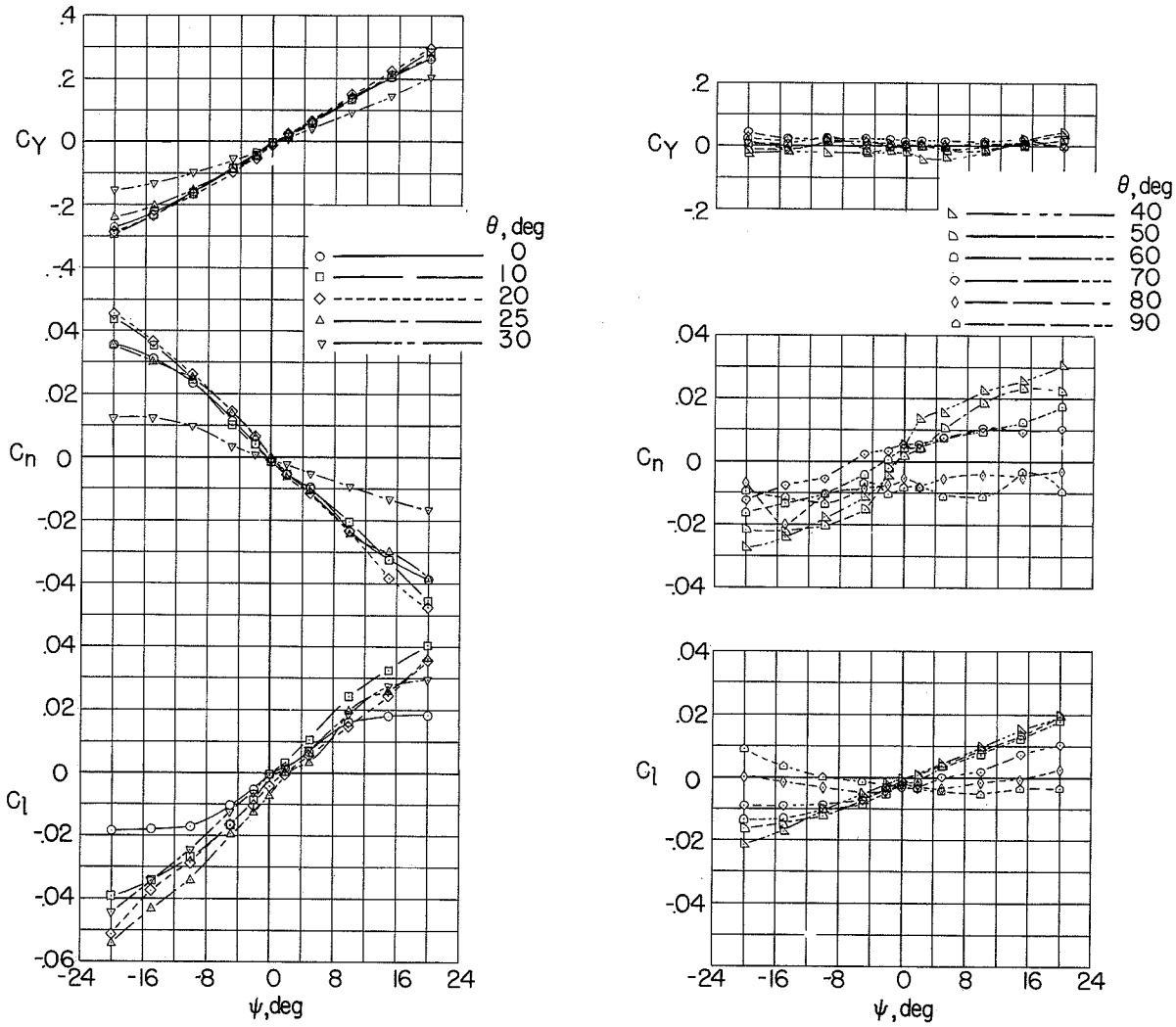

(b) Top vertical tail on.

Figure 5.- Continued.

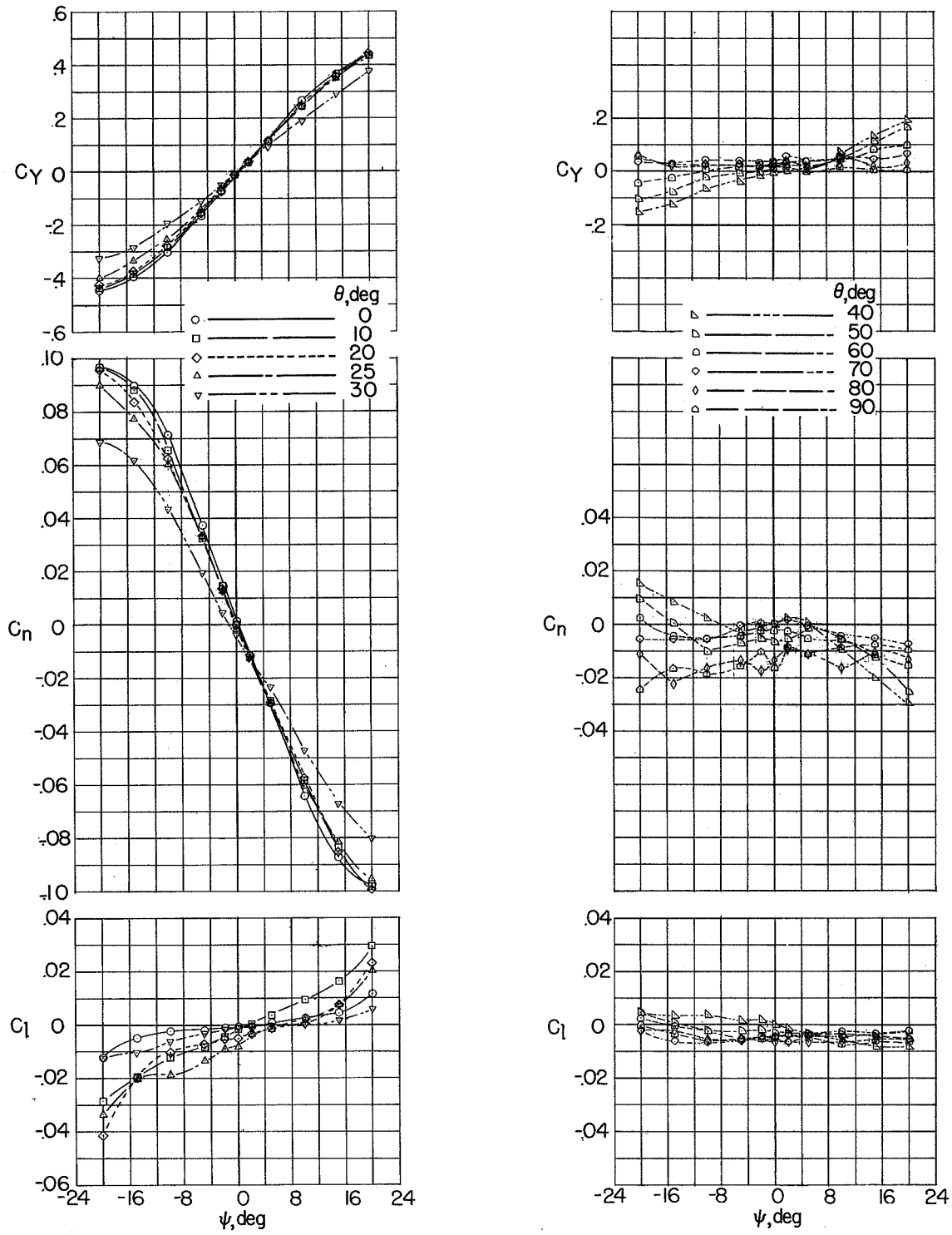

(c) Top and bottom vertical tails on.

Figure 5.- Concluded.

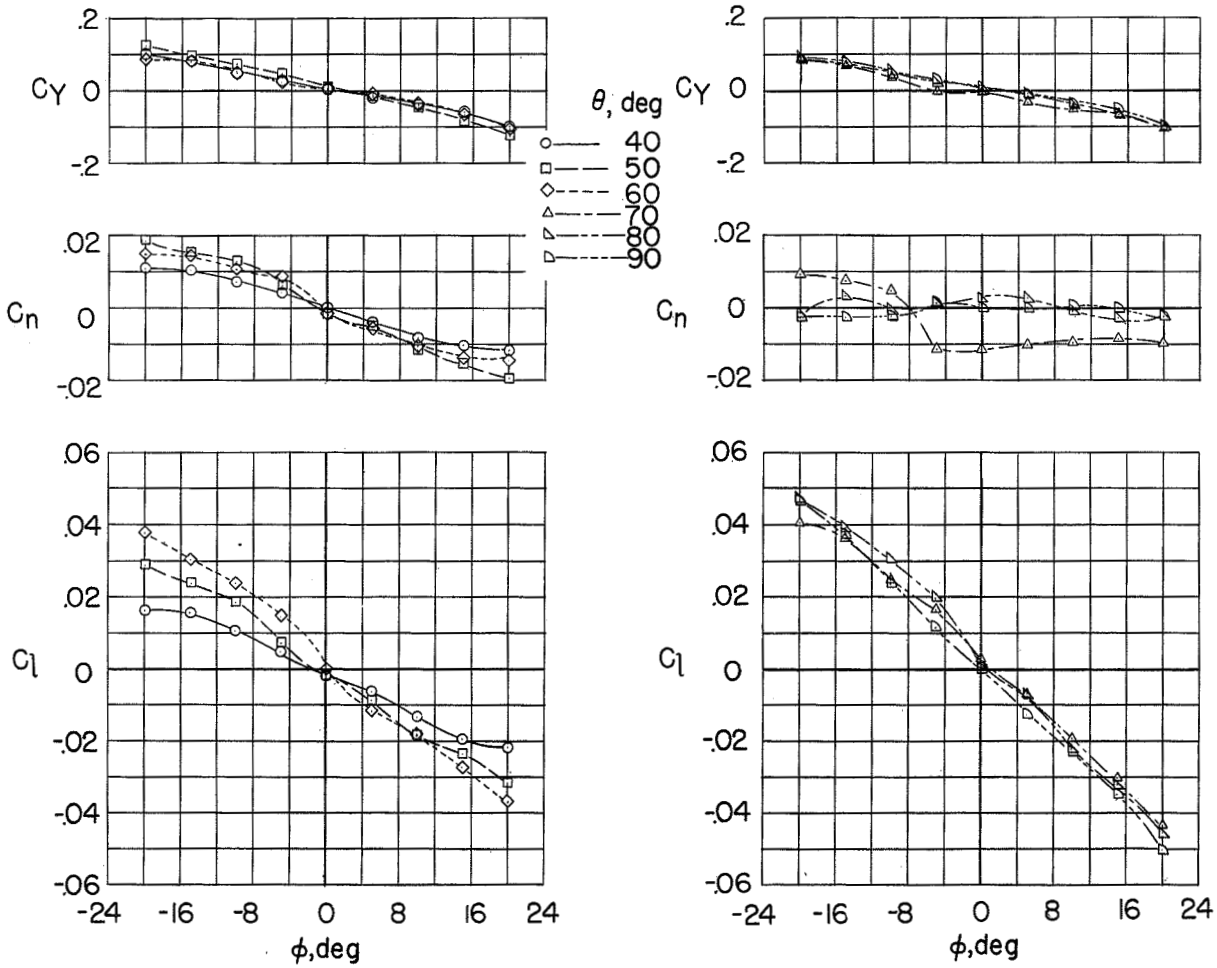

(a) Vertical tails off.

Figure 6.- Variation of the static lateral stability coefficients with angle of roll. $\psi = 0^{\circ}$.

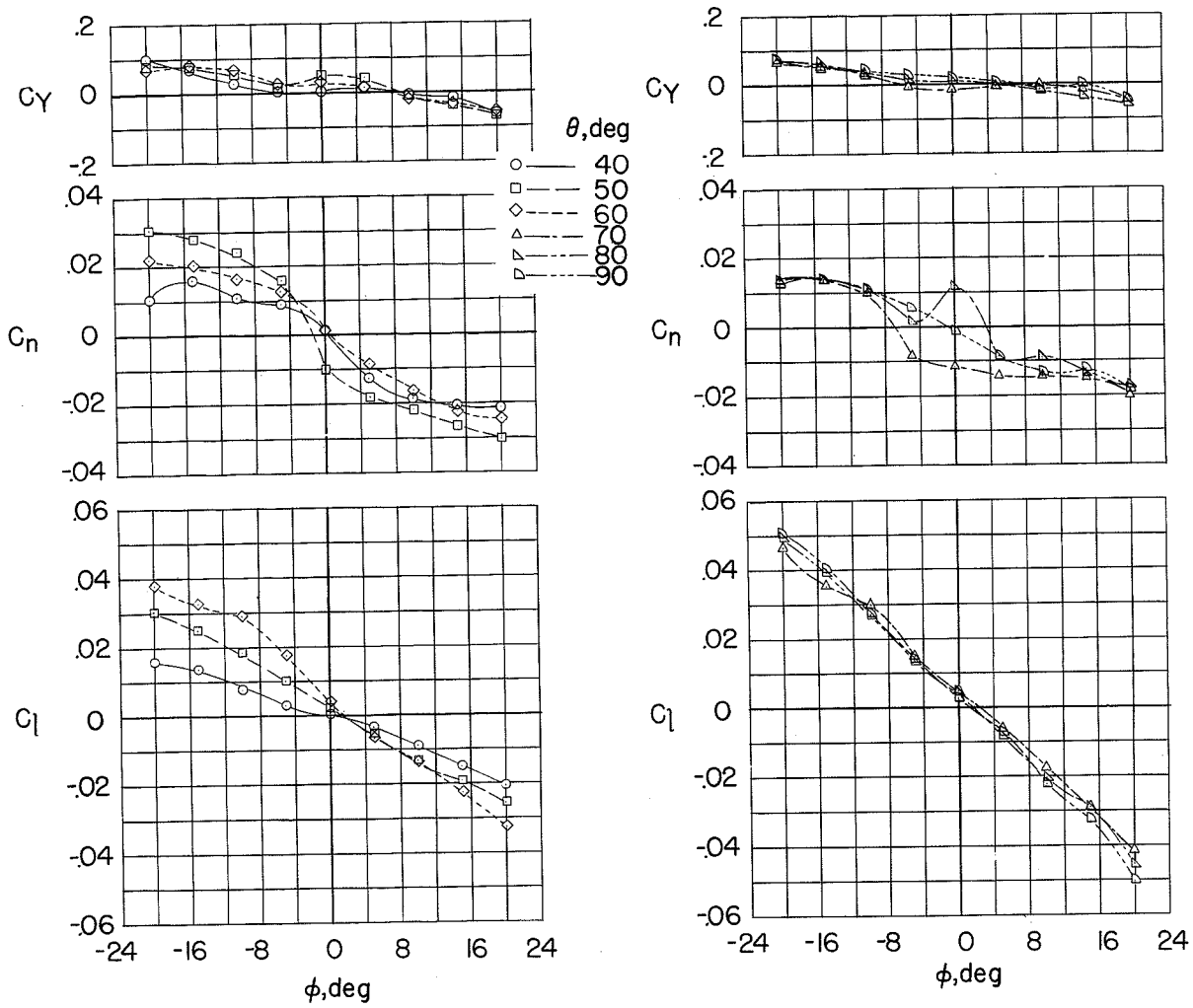

(b) Top vertical tail on.

Figure 6.- Continued.

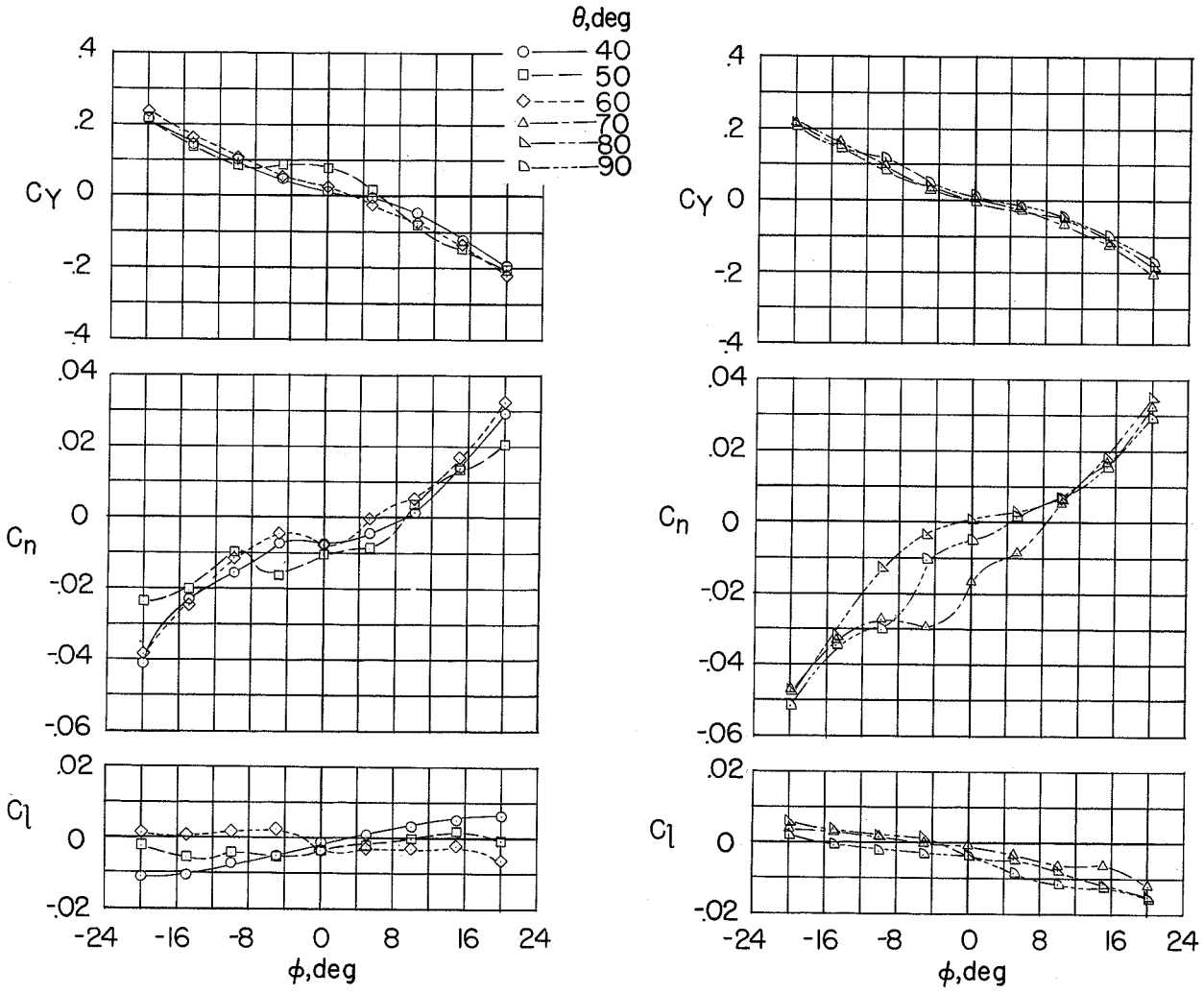

(c) Top and bottom vertical tails on.

Figure 6.- Concluded.

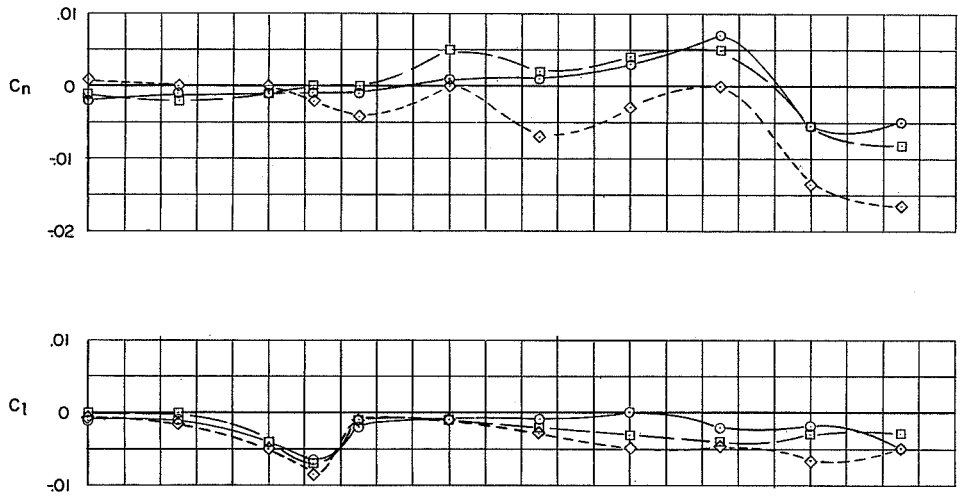

(a) Data from figure 5.

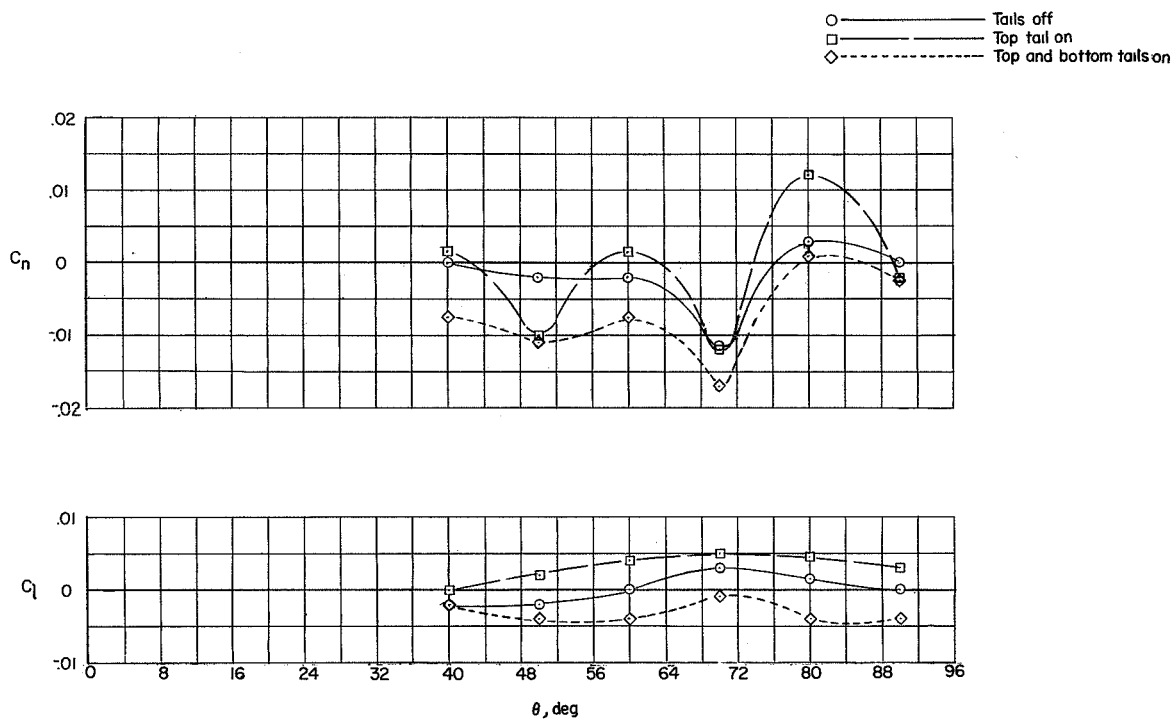

(b) Data from figure 6.

Figure 7.- Variation of yawing- and rolling-moment coefficients with angle of pitch. $\psi = 0^{\circ}$; $\phi = 0^{\circ}$.

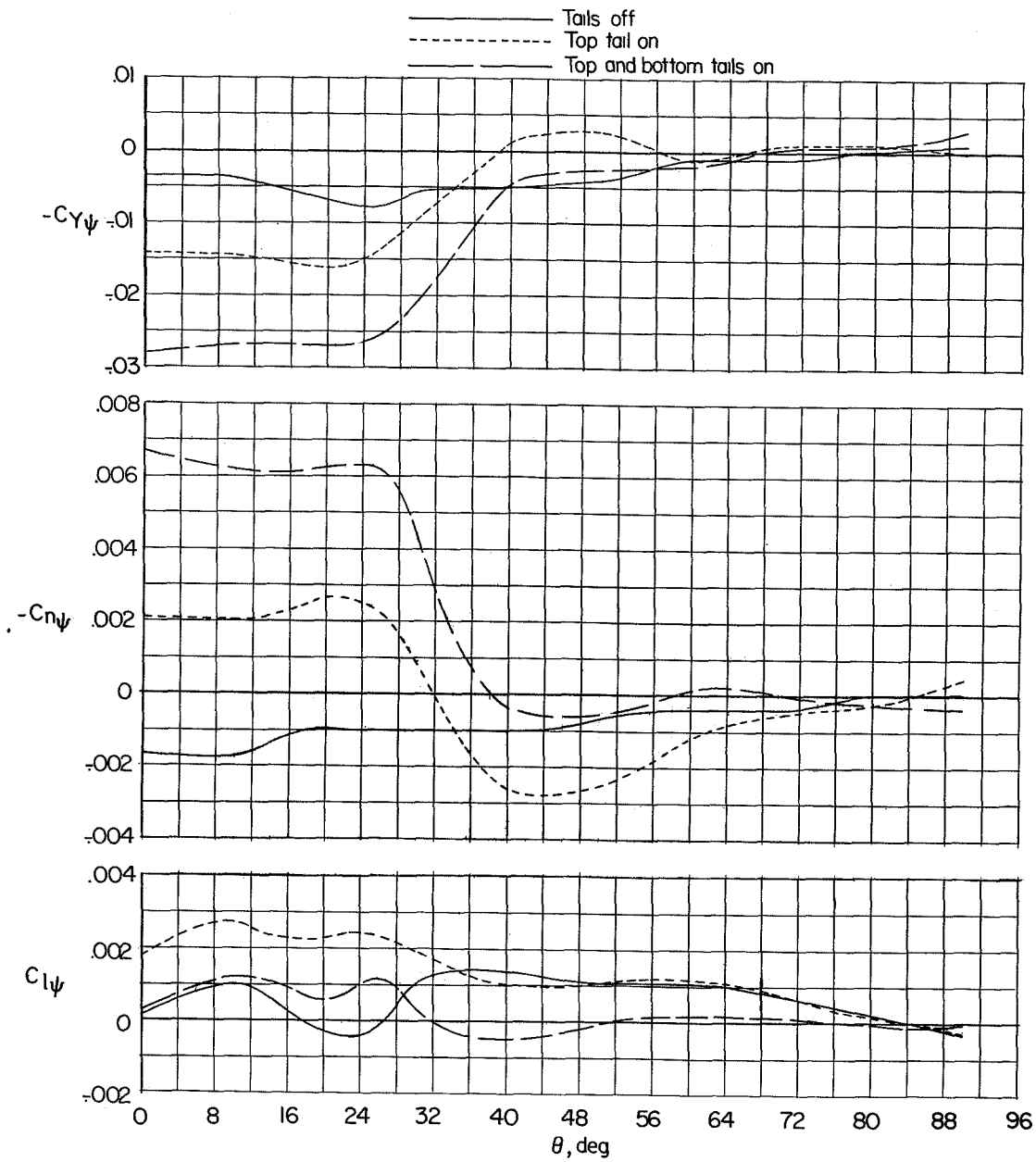

Figure 8.- Variation of the static yaw derivatives with angle of pitch. $\phi = 0^{\circ}$.

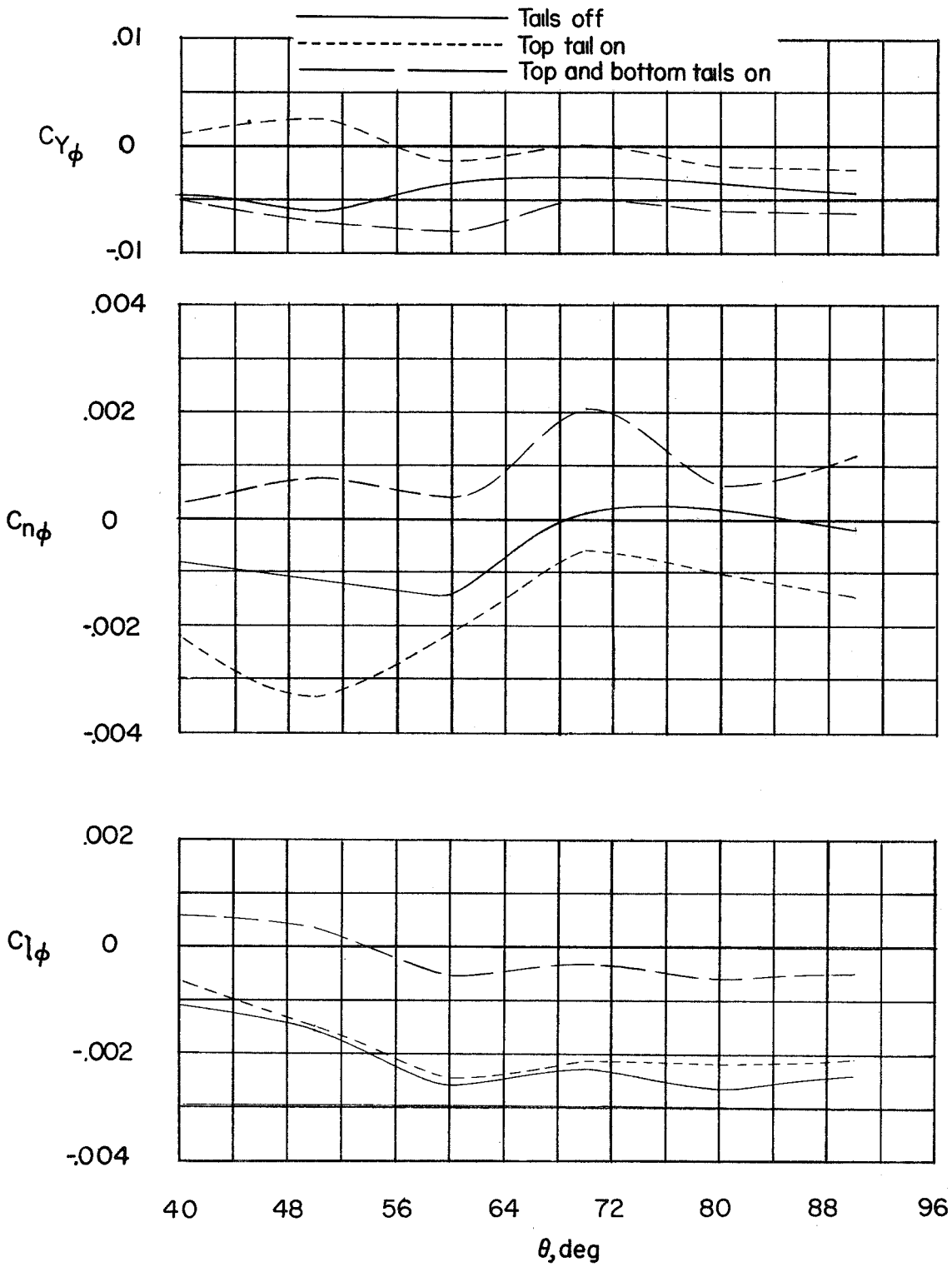

Figure 9.- Variation of the static roll derivatives with angle of pitch. $\psi = 0^{\circ}$.

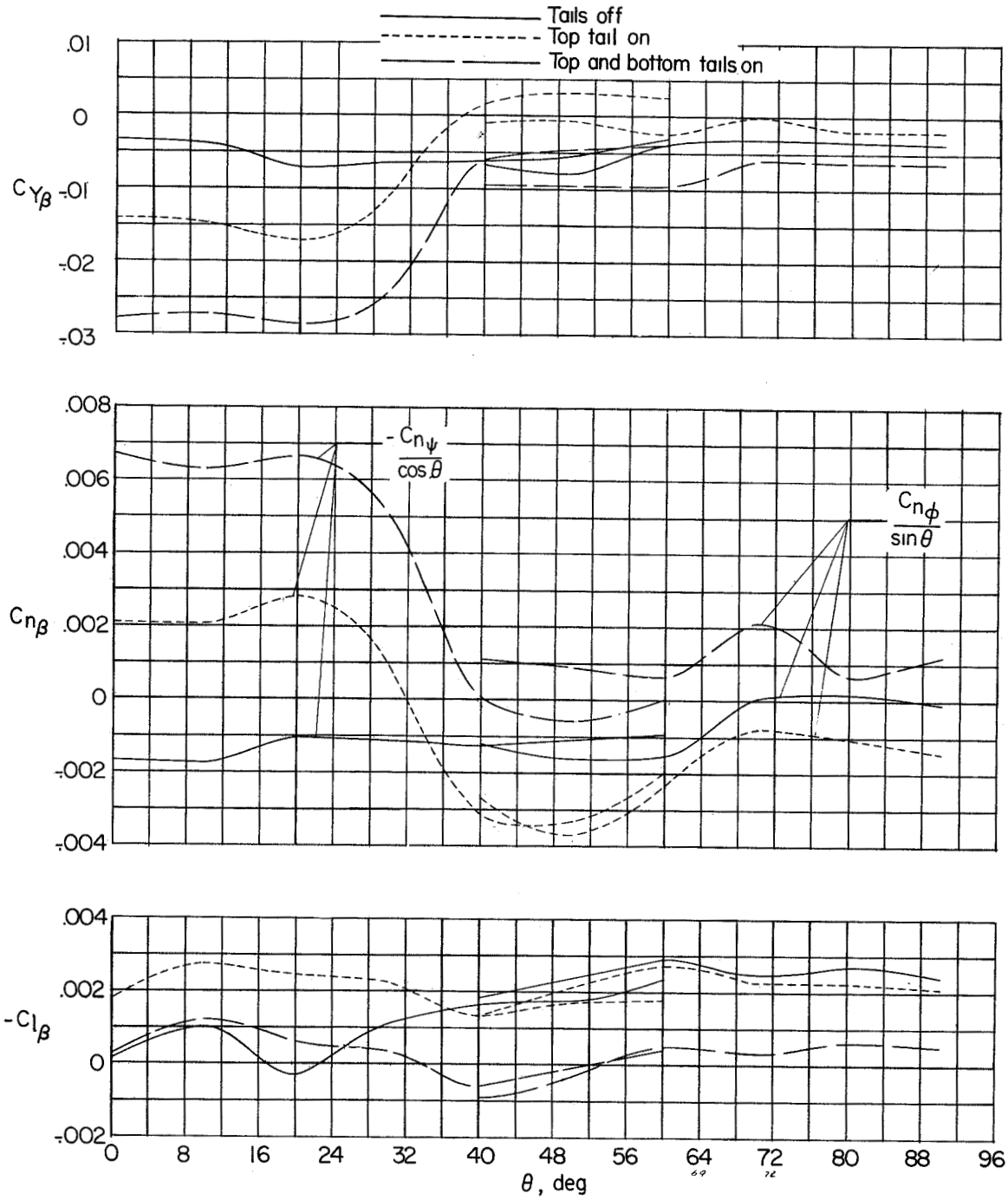

Figure 10.- Variation of the sideslip derivatives with angle of pitch.

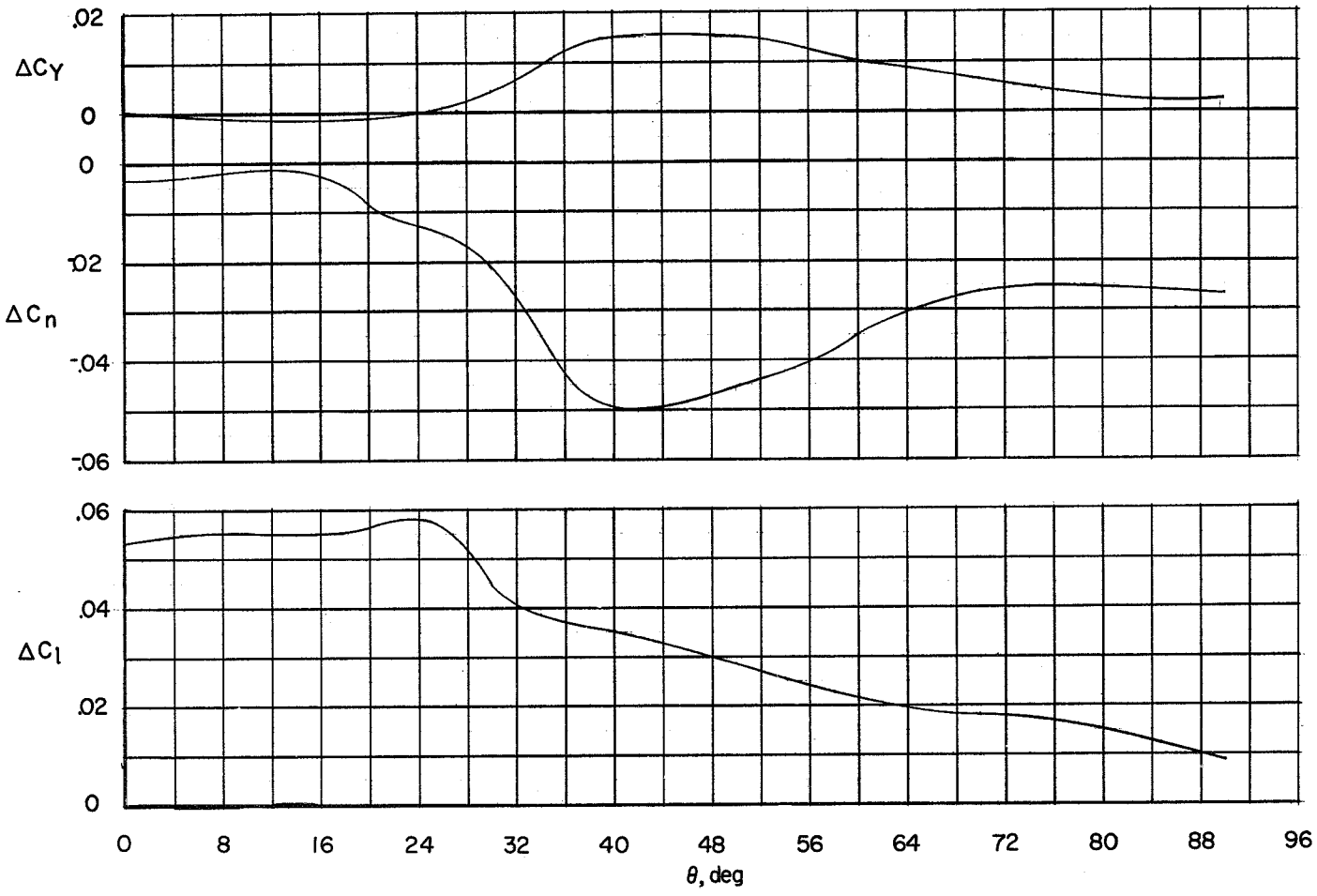

(a) Ailerons deflected 60° total. $\delta_r = 0^\circ$ $\left(\delta_{a_l} = 30^\circ \text{ and } \delta_{a_r} = -30^\circ\right)$.

Figure 11.- Increments in the lateral-force and moment coefficients produced by deflections of the ailerons and rudders. Top and bottom tails on.

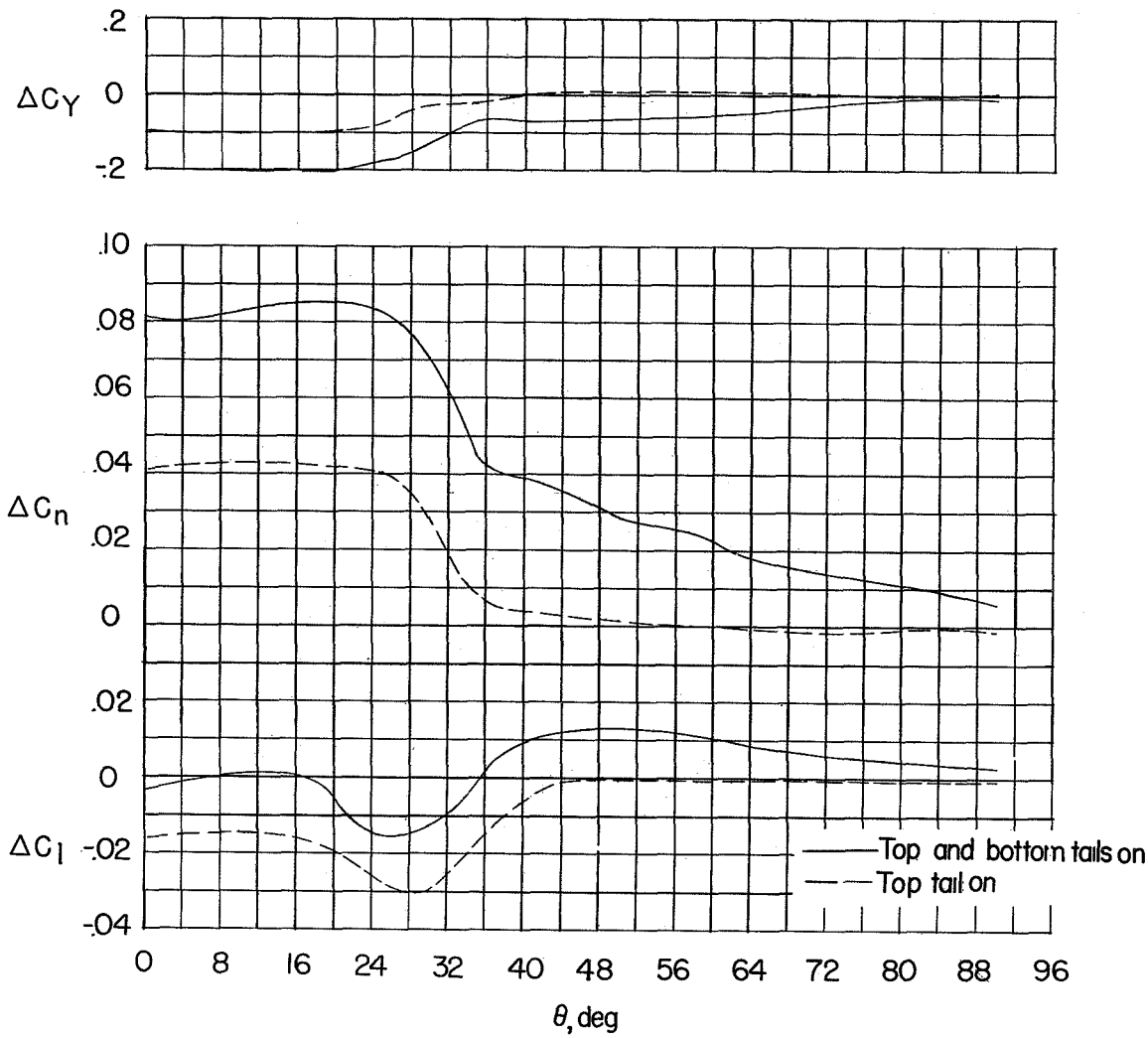

(b) Rudders deflected -20°. $\delta_a = 0°$.

Figure 11.- Concluded.

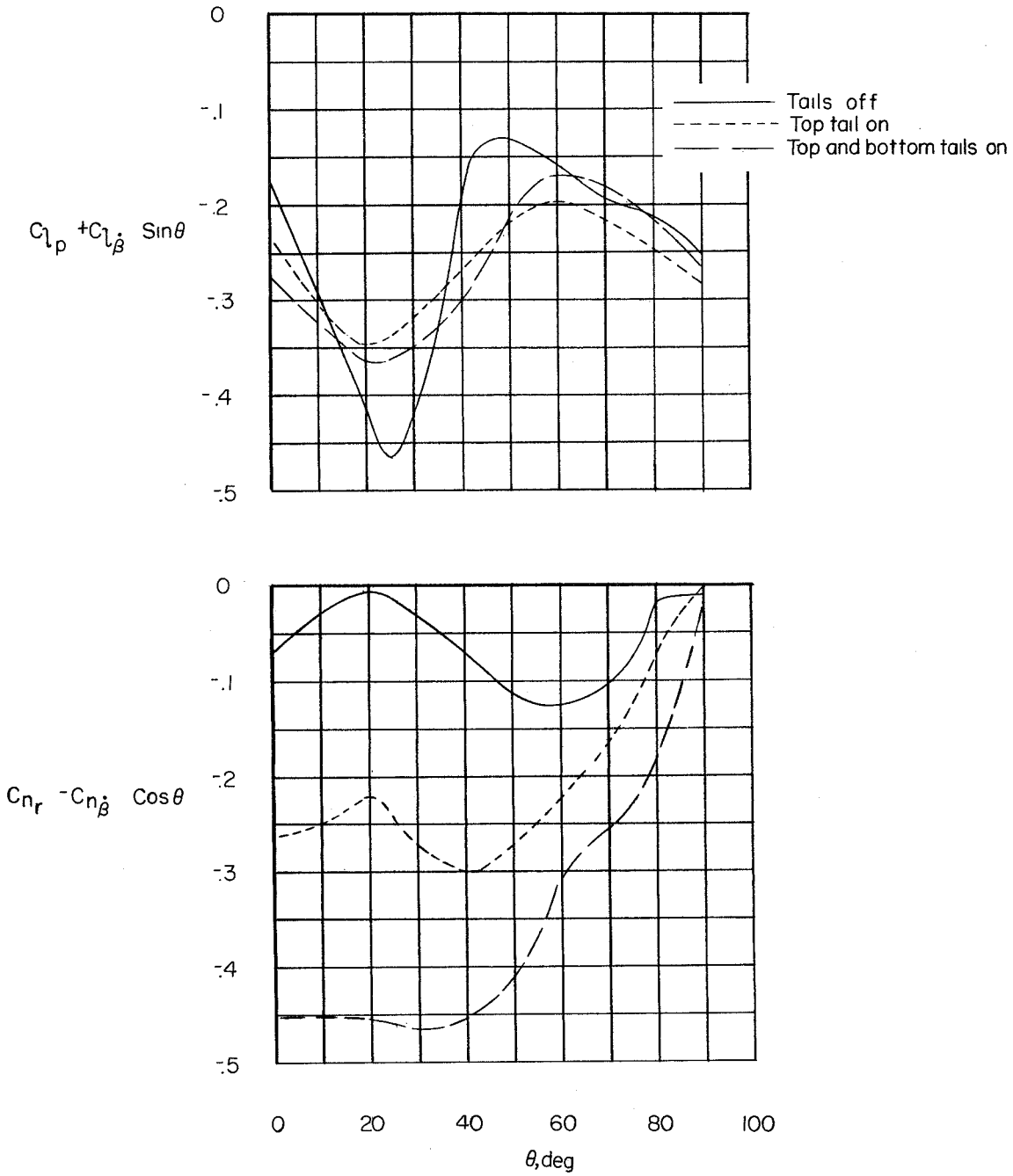

Figure 12.- Variation of the damping in roll and damping in yaw with angle of pitch.

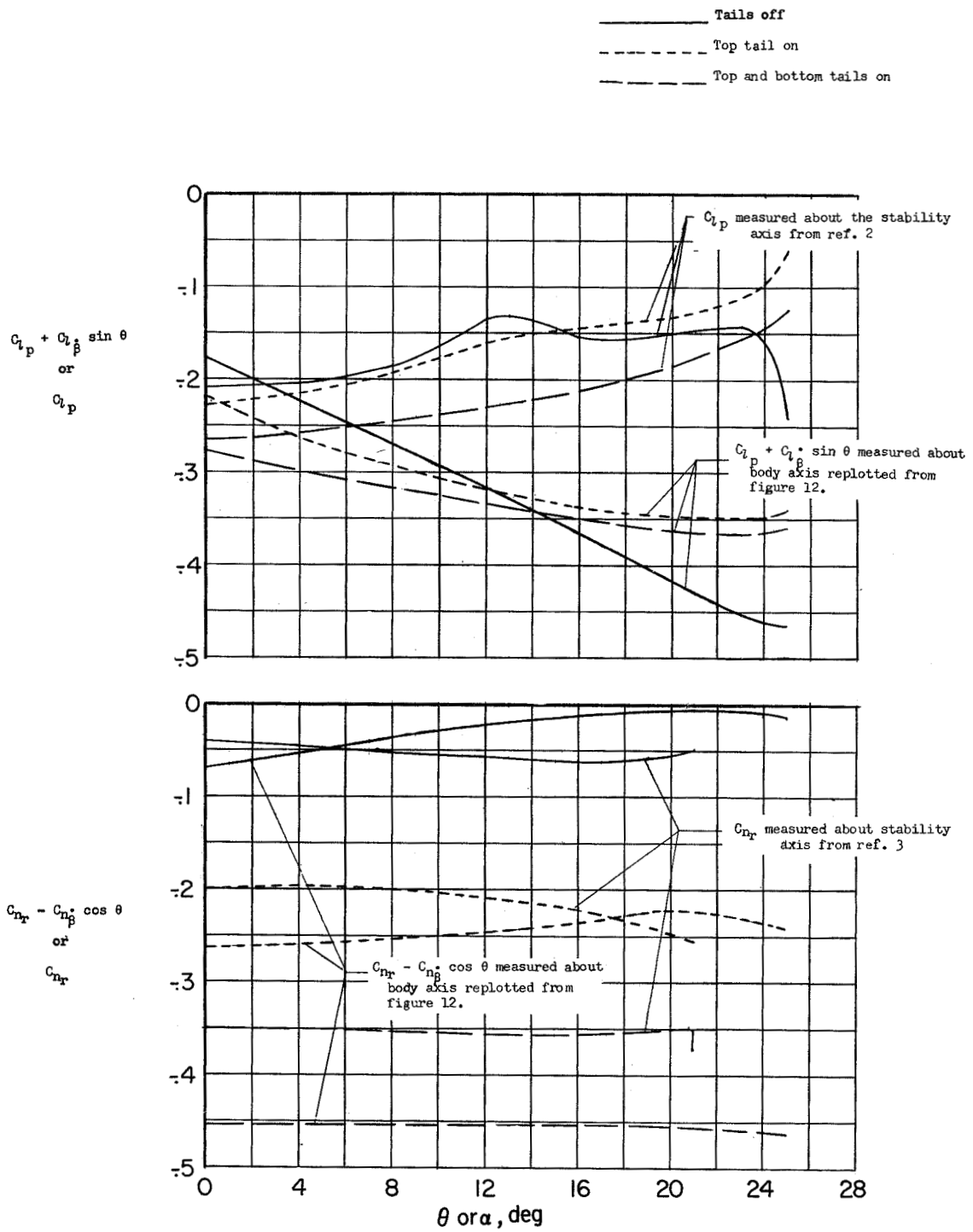

Figure 13.- Damping in roll and damping in yaw measured about stability axes and body axes.

NACA-Langley - 9-29-54 - 50

CONFIDENTIAL
Restriction/Classification Cancelled

CONFIDENTIAL
Restriction/Classification Cancelled